Physics Letters B 746 (2015) 127–131

Contents lists available at ScienceDirect

Physics Letters B

www.elsevier.com/locate/physletb

Data on I^s and I^c in $\vec{\gamma}\, p \to p\pi^0\pi^0$ reveal cascade decays of $N(1900)$ via $N(1520)\pi$

CBELSA/TAPS Collaboration

V. Sokhoyan [a,*], E. Gutz [a,b], H. van Pee [a], A.V. Anisovich [a,c], J.C.S. Bacelar [d], B. Bantes [e], O. Bartholomy [a], D. Bayadilov [a,c], R. Beck [a], Y. Beloglazov [c], R. Castelijns [d], V. Crede [f], H. Dutz [e], D. Elsner [e], R. Ewald [e], F. Frommberger [e], M. Fuchs [a], Ch. Funke [a], R. Gregor [b], A. Gridnev [c], W. Hillert [e], Ph. Hoffmeister [a], I. Horn [a], I. Jaegle [g], J. Junkersfeld [a], H. Kalinowsky [a], S. Kammer [e], V. Kleber [e], Frank Klein [e], Friedrich Klein [e], E. Klempt [a], M. Kotulla [b,g], B. Krusche [g], M. Lang [a], H. Löhner [d], I. Lopatin [c], S. Lugert [b], T. Mertens [g], J.G. Messchendorp [d], V. Metag [b], M. Nanova [b], V.A. Nikonov [a,c], D. Novinski [c], R. Novotny [b], M. Ostrick [e], L. Pant [b], M. Pfeiffer [b], D. Piontek [a], A. Roy [b], A.V. Sarantsev [a,c], Ch. Schmidt [a], H. Schmieden [e], S. Shende [d], A. Süle [e], V.V. Sumachev [c], T. Szczepanek [a], A. Thiel [a], U. Thoma [a], D. Trnka [b], R. Varma [b], D. Walther [a], Ch. Wendel [a], A. Wilson [a,f]

[a] Helmholtz–Institut für Strahlen- und Kernphysik, Universität Bonn, 53115 Bonn, Germany
[b] II. Physikalisches Institut, Universität Gießen, 35392 Gießen, Germany
[c] Petersburg Nuclear Physics Institute, Gatchina, 188300, Russia
[d] Kernfysisch Versneller Instituut, Groningen, The Netherlands
[e] Physikalisches Institut, Universität Bonn, 53115 Bonn, Germany
[f] Department of Physics, Florida State University, Tallahassee, FL 32306, USA
[g] Departement Physik, Universität Basel, 4056 Basel, Switzerland

ARTICLE INFO

Article history:
Received 27 February 2015
Received in revised form 14 April 2015
Accepted 28 April 2015
Available online 30 April 2015
Editor: D.F. Geesaman

Keywords:
Baryon spectroscopy
Double meson photoproduction
Polarization observables

ABSTRACT

Photoproduction of two neutral pions off the proton is studied using linearly polarized photons, and the polarization observables I^s and I^c are measured for the first time. These two observables are unique to multi-meson final states; they characterize correlations between the linear photon polarization and the direction of outgoing single particles in photoproduction of three-body final states. The I^s and I^c distributions suggest that, in the 1.8 to 2.0 GeV mass region, the $N(1520)3/2^-\pi$ intermediate state is reached with reaction dynamics consistent with a dominant $J^P = 3/2^+$ wave. These data are included in the Bonn–Gatchina (BnGa) partial wave analysis which is based on a large variety of data; the analysis confirms a significant contribution from the reaction chain $\gamma p \to N(1900)3/2^+ \to N(1520)3/2^-\pi^0 \to p\pi^0\pi^0$.

1. Introduction

The properties of excited states of the nucleon carry information on its constituents and their interactions, particularly on the interaction between quarks and gluons in the confinement regime of QCD. The majority of nucleon and Δ excitations listed in the Review of Particle Physics (RPP) [1] were discovered in partial wave analyses of πN elastic scattering experiments. However, a large fraction of the resonances reported by Höhler and by Cutkosky and their collaborators [2,3] were not confirmed in a later analysis based on a much larger data sample [4]. Quark models [5,6] and lattice QCD [7] predict even more resonances than have been observed in [2,3]. Obviously, there is a large number of resonances with weak coupling to πN which cannot be extracted

* Corresponding author.
E-mail addresses: sokhoyan@uni-mainz.de (V. Sokhoyan), klempt@hiskp.uni-bonn.de (E. Klempt).

http://dx.doi.org/10.1016/j.physletb.2015.04.063

reliably from πN elastic scattering data. Excitation of resonances with isospin $I = 1/2$ (N^*) or $I = 3/2$ (Δ^*) in photo-induced reactions holds the promise to unravel these states and to identify the dynamics leading to the excitation spectrum [8–10]. The excited states of the nucleon are, however, extremely short-lived, rendering their identification very difficult. Mostly, several resonances overlap; the production amplitudes interfere and thus, the resulting angular distributions are rather complicated. Exception is the well-known $\Delta(1232)$ which dominates the low-energy region in single-pion production: its $\Delta(1232) \to N\pi$ decay angular distribution reveals the spin-parity $J^P = 3/2^+$. Likewise, $N(1535)$ with $J^P = 1/2^-$ dominates the reaction $\gamma N \to N\eta$, and a flat decay angular distribution is observed as expected for spin 1/2. All other resonances require complicated partial wave analyses (PWAs) to determine their spin and parity (even though $\Delta(1232)$ and $N(1535)1/2^-$ require a PWA as well to establish their existence and properties).

In this Letter we present new data on $\vec{\gamma} p \to p\pi^0\pi^0$ using linearly polarized photons inducing a spin alignment of intermediate states. This alignment leads to a characteristic decay pattern which depends on the quantum numbers of the intermediate state. In the 1.8–2.0 GeV mass region, the decay pattern indicates dominance of the $3/2^+$ partial wave decaying into $N(1520)3/2^-\pi^0$. No partial wave analysis is required to arrive at this conclusion, even though it is confirmed in a partial wave analysis. We assign it to the reaction chain $\gamma p \to N(1900)3/2^+$ with $N(1900)3/2^+$ decaying via $N(1520)3/2^-\pi^0$ as an intermediate isobar. We mention that this resonance – suggested in [11] and not seen in [2–4] – is clearly seen in $\gamma p \to \Lambda K^+$ [12]. It is one of the two resonances (with $N(1875)3/2^-$) which are listed in the Baryon Summary Table of the RPP [1] now as three-star (existence very likely) resonances due to their observation in photoproduction. This resonance is of particular importance since it can be assigned to a quartet of resonances which are inconsistent with a simple quark–diquark picture of baryon excitations with diquarks frozen in their S-wave [13]. Further confirmation of this resonance is hence highly desirable.

2. The experiment

Electrons of energy 3200 MeV were ejected from the ELectron Stretcher Accelerator (ELSA) [14] to produce an energy-tagged linearly polarized photon beam using coherent bremsstrahlung off a diamond radiator. Two different polarization settings yielded maximum polarizations of 49.2% for 1300 MeV photons and 38.7% for 1600 MeV, respectively [15,16]. After the bremsstrahlung process, the electrons were momentum analyzed using a dipole magnet in combination with a scintillator hodoscope. The photons impinged on a 5 cm long liquid hydrogen target, located in the center of the CBELSA/TAPS detector setup. It consists of two electromagnetic calorimeters, the Crystal Barrel [17] with 1290 CsI(Tl) crystals and the TAPS detector in a forward-wall setup with 528 BaF_2 modules [18]. The two calorimeters cover the complete azimuthal angle and polar angles from 6° to 168°, leading to a total solid angle coverage of more than 98%. Additional information on charged particles is provided by a three-layer scintillating fiber detector surrounding the target and by scintillator plates in front of the TAPS crystals. For further details, see [19].

To select $p\pi^0\pi^0$ events, events with four or five distinct hits in the calorimeters were retained for analysis. The invariant masses of two pairs of these hits – assumed to be photons – had both to agree with the π^0-mass within ±35 MeV and their missing mass had to be consistent with the proton mass within ±100 MeV. For the five-hit events the missing proton direction, calculated from the missing momentum and assuming that the proton originated from the target center, had to match the fifth hit (within ±10° in the azimuthal angle; within ±5° in the polar angle for TAPS, within ±10° for the Crystal Barrel). The maximum energy deposited in the calorimeters by proton candidates had to be compatible with the limits derived from Monte Carlo simulations as well as the maximum number of crystals belonging to a proton cluster. The polar angle had to be smaller than the maximum polar angle kinematically allowed for protons. For events with four hits in the calorimeter, one of the following conditions had to be fulfilled: i) for missing momenta below the minimum detection threshold of the Crystal Barrel calorimeter an additional signal in the inner detector had to agree with the missing particle within ±15° in ϕ and within ±20° in θ; ii) the direction of the momentum of the missing proton had to be consistent with the forward hole in TAPS; or iii) the momentum had to be sufficiently small so that the proton may have not been detected in any of the detectors. Next, the data were subjected to a kinematic fit [20], imposing energy and momentum conservation. The proton direction resulting from the fit had to agree with the direction of the proton reconstructed in one of the calorimeters if available. Events that exceeded a Confidence Level (CL) of 10% for the $\gamma p \to p\pi^0\pi^0$ hypothesis were retained, events with a CL for $\gamma p \to p\pi^0\eta$ exceeding the CL for $\gamma p \to p\pi^0\pi^0$ were rejected. After all cuts, the data sample contains about 560 000 events in the photon energy range of 970 to 1650 MeV with a background contamination over the full energy range of below 1%.

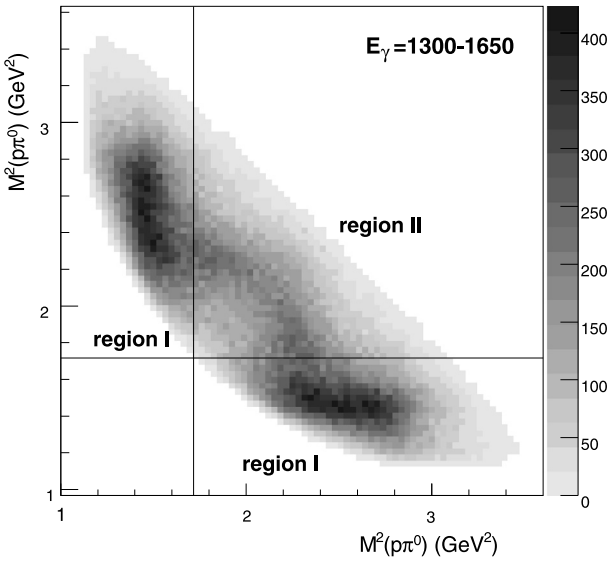

Fig. 1. The Dalitz plot for the reaction $\gamma p \to p\pi^0\pi^0$ is divided into two regions by a cut at $m_\Delta + 2\Gamma_\Delta/3$, a $\Delta(1232)$ (I) and an $N(1520)3/2^-$ (II) region.

Fig. 1 shows the $p\pi^0\pi^0$ Dalitz plot for photons of 1300 to 1650 MeV, corresponding to a center-of-mass energy of 1820 to 2000 MeV; further distributions and a full account of the partial wave analysis can be found elsewhere [21]. The Dalitz plot shows uncorrected experimental data, without including the subsequent corrections for detector acceptance and incident photon flux. Since the two neutral pions are identical, there are two entries per event; therefore the Dalitz plot is symmetric with respect to the diagonal. The largest contributions are seen at $M^2_{p\pi^0}$ around 1.5 GeV^2 stemming from $\Delta(1232)$ as an intermediate state. Less pronounced bands can be seen at $M^2 \approx 2.25$ GeV^2 or $M \approx 1.5$ GeV. The PWA fit returns mass and width of $M_{\text{pole}} = 1507 \pm 2$ MeV, $\Gamma = 111 \pm 3$ MeV, compatible with the PDG values for $N(1520)3/2^-$ ($\approx 1510, \approx 110$ MeV).

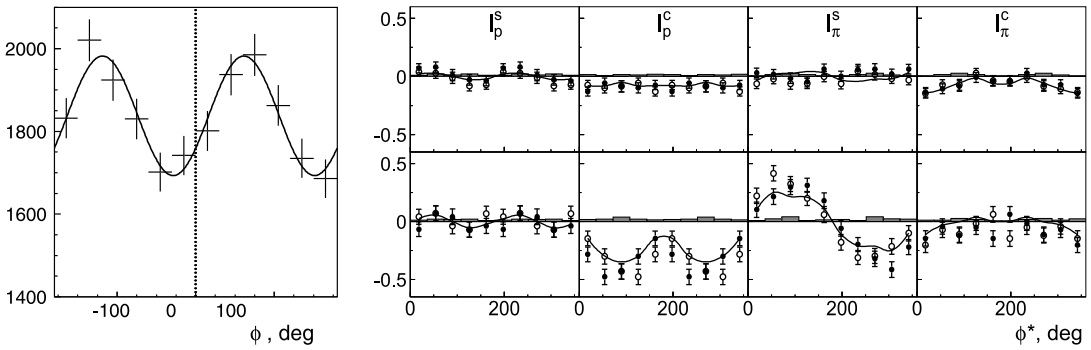

Fig. 2. Left: Example of a ϕ-distribution of the recoiling pion in the region $18° \le \phi^* \le 36°$ for an incoming energy range $970 < E_\gamma < 1200$ MeV. Right: I^s_p, I^c_p, I^s_π, and I^c_π as functions of ϕ^* for $1300 < E_\gamma < 1650$ MeV. The four subfigures on the first (second) row show the distributions for events in region I (II) of the Dalitz plot (Fig. 1). Dots: I^s, I^c; open circles: mirror points due to symmetry (see text); grey band: syst. errors. The solid curve represents the BnGa PWA fit.

3. Polarization observables

Two-meson production is not restricted to a single plane but three planes can be defined: the photon plane, defined by the incoming photon and its polarization; the production plane spanned by the direction of the incoming photon and one of the outgoing particles; and the decay plane defined using the other two final-state particles. The angle between a production plane and the photon plane, with an offset of 90°, is called ϕ. The decay plane and the production plane enclose an angle ϕ^*. With these angles, the cross section adopts the form [22]

$$\frac{d\sigma}{d\Omega} = \left(\frac{d\sigma}{d\Omega}\right)_0 \{1 + P_l[I^s \sin(2\phi) + I^c \cos(2\phi)]\}. \quad (1)$$

Here, $\left(\frac{d\sigma}{d\Omega}\right)_0$ is the cross section with no polarization, and P_l is the degree of linear photon polarization. I^s and I^c are extracted by a fit to the ϕ-distributions. Depending on the choice of the production plane, the distributions I^s_p, I^c_p, I^s_π, I^c_π can be derived. An example for a ϕ-distribution is shown in Fig. 2, left. Both, the $\cos(2\phi)$-modulation due to I^c and the $\sin(2\phi)$-modulation due to I^s – resulting in a displacement of the minima off the dotted line – are clearly visible.

I^s and I^c fulfill some symmetry requirements which can be used to check the consistency of the data. I^s, I^c can be written as functions of ϕ^* [19] in the form $I^s(\phi^*) = \sum_n a_n \sin(n\phi^*)$, and $I^c(\phi^*) = \sum_n b_n \cos(n\phi^*)$. The transformation $\phi^* \to 2\pi - \phi^*$ yields $I^s(2\pi - \phi^*) = -I^s(\phi^*)$ and $I^c(2\pi - \phi^*) = I^c(\phi^*)$. In the proton recoiling case, due to the indistinguishability of π^0 s, additional symmetry conditions $I^s(\phi^*) = I^s(\phi^* + \pi)$ and $I^c(\phi^*) = I^c(\phi^* + \pi)$ occur. In the data, these requirements are met within the statistical uncertainties.

Fig. 2, right, shows these four observables, integrated over $\cos\theta_p$ and as functions of ϕ^*, for the two regions I and II of the Dalitz plot (Fig. 1). The four subfigures in the first line show the I^s and I^c distributions for events in the $\Delta(1232)$ region (region I, $M_{p\pi^0} \le m_\Delta + 2\Gamma_\Delta/3$). The distributions show no significant structure, the data points are all close to zero. We interpret this observation by assuming that there are many resonances decaying via $\Delta(1232)\pi$ – leading to different I^s_p, I^c_p, I^s_π, I^c_π distributions with positive or negative sign so that their sum gives a result close to zero.

For the present discussion, we are interested in events where the $N(1520)3/2^-$ resonance contributes to the decay chain as an intermediate state. The four subfigures in the second line in Fig. 2, right, show I^s and I^c for events in region II of the Dalitz plot where both proton–pion invariant masses are compatible with $N(1520)3/2^-$. These distributions show significant deviations from zero. This may indicate that there is one leading partial wave which produces this pattern. Hence we study region II more carefully.

Fig. 3, left, shows the I^c_p as a function of ϕ^* for three bins in photon energy and four bins in $\cos\theta_p$. The error bars reflect the statistical errors. The systematic uncertainty due to the lack of detection efficiency for certain regions of the phase space was derived from the difference between predictions of the Bonn–Gatchina PWA obtained for generated and reconstructed Monte Carlo events. This difference was compared to the effect of the two dimensional phase space acceptance correction (with ϕ, ϕ^* as coordinates), and the largest effect was taken as the systematic uncertainty. I^c_p adopts negative values. In the low energy bins, the mean value is close to -0.25; it corresponds to the two-body beam asymmetry Σ_p. The better description of the experimental data for $1450 < E_\gamma < 1650$ MeV (and $\cos\theta_p > 0$) by fits which include the $N(1900)3/2^+$ provides the first suggestive evidence for the existence of this resonance. For these two bins we find $\chi^2_{\text{data}} = 11/20$ (36/20) for the fit with (without) $N(1900)3/2^+$. Note that the dashed curve in the $0 < \cos\theta_p < 0.5$ bin stays in the grey area.

In the $1300 < E_\gamma < 1650$ MeV energy range, the Particle Data Group [1] lists N^* and Δ^* resonances with $J^P = 1/2^+, 3/2^+, 5/2^+, 7/2^+, 1/2^-, 3/2^-, 5/2^-$. We now identify $J^P = 3/2^+$ as dominating partial wave in this photon energy range. The I^s and I^c data presented in the second line of Fig. 2, right, are shown repeatedly in Fig. 3, right. The data are compared to a series of very simple model predictions: Each model assumes that in this photon energy range, the reaction $\gamma p \to p\pi^0\pi^0$ is due to the production of one single resonance produced in the reaction $\gamma p \to N(1520)3/2^-\pi^0$, with $N(1520)3/2^-$ decaying into $p\pi^0$. There are at most two parameters which determine I^s and I^c in this reaction chain: the ratio of the two helicity amplitudes $A_{1/2}/A_{3/2}$ of the chosen resonance, and the ratio of the decay amplitudes with high and low orbital angular momenta, D/S, F/P, or G/D. For resonances with $J^P = 1/2^\pm$, there is only one helicity amplitude, and their contribution to I^s and I^c vanishes.

In the two-parameter fit to the data, the χ^2 per data point is 1.2 for the hypothesis that the initial state is purely in the $J^P = 3/2^+$ wave and decays into $N(1520)3/2^-\pi$ with $D/S = 0.05$. For this hypothesis, the fit returns a helicity ratio $A_{1/2}/A_{3/2} \approx -0.47$. For the other initial waves, the χ^2 is per data point is between 5 and 10. These observations strongly suggest that a baryon resonance with $J^P = 3/2^+$ quantum numbers is formed. The resonance could be $N(1900)3/2^+$ or $\Delta(1920)3/2^+$. We note that $N(1900)3/2^+$ has a negative, $\Delta(1920)3/2^+$ a positive helicity ratio, the RPP [1] lists $A_{1/2}/A_{3/2} \approx -0.55$ and $+1.7$, respectively. We

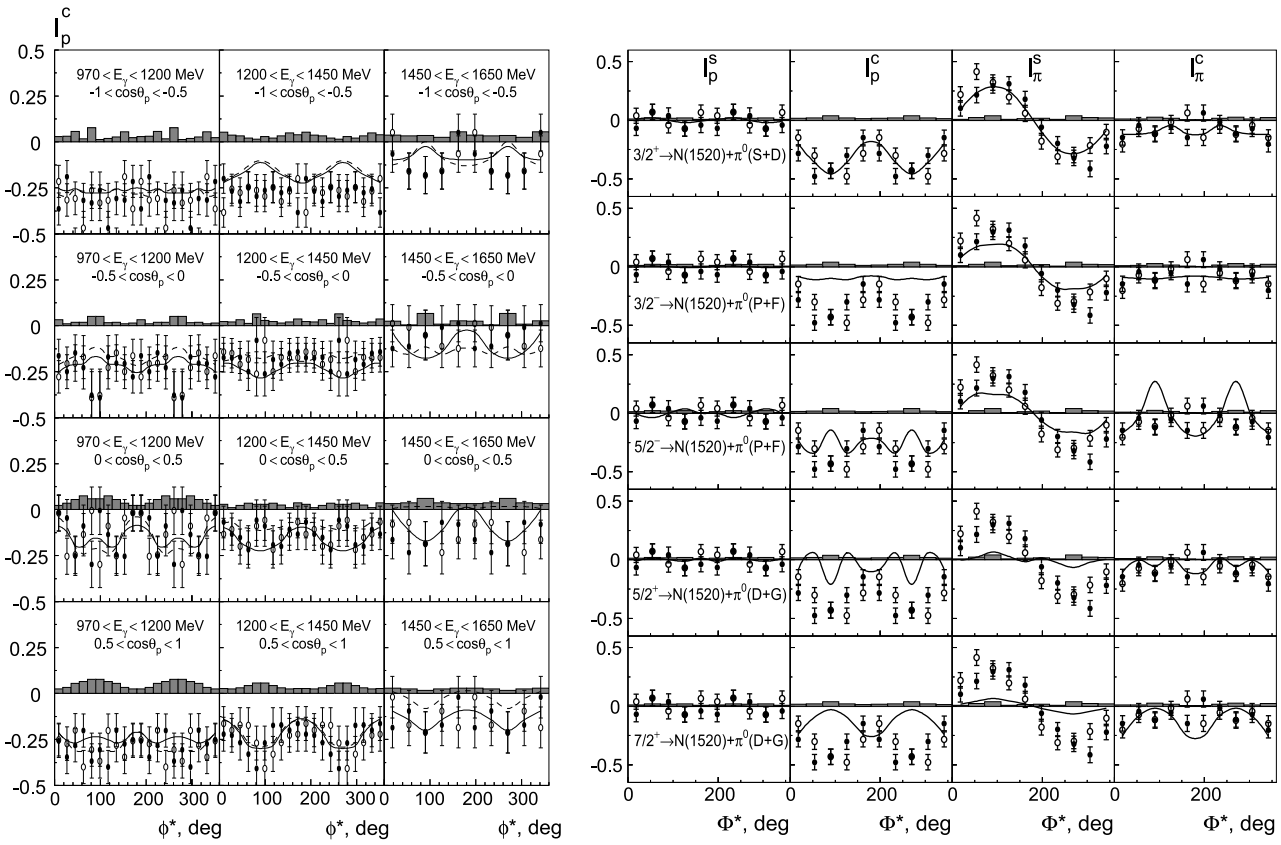

Fig. 3. Left: The polarization observable I^c_p, data, and BnGa PWA fit with (solid curve) and without (dashed curve) $N(1900)3/2^+$ as a function of ϕ^* for 3 bins in E_γ and 4 bins in $\cos\theta_p$. Right: I^s and I^c for events in region II (Fig. 1). Solid symbols: extracted directly from the data, open symbols: mirror points due to symmetry (see text). The grey areas represent the systematic errors. The data are shown repeatedly and compared to simulated distributions for the reaction chains $(J^P) \to N(1520)3/2^- + \pi^0$. Distributions for $(1/2^\pm) \to N(1520)3/2^- + \pi^0$ vanish and are not shown. In the fits, the systematic errors are added quadratically to the statistical errors. See Fig. 2 for symbols.

Table 1
Properties of $N(1900)3/2^+$. Masses and widths are given in MeV, $A^{1/2}$ and $A^{3/2}$ in GeV$^{-1/2}$. The values given in [12,23,32,33] are reproduced as small numbers.

M_{BW}	1910 ± 30	Γ_{BW}	270 ± 50
1915 ± 60; 1905 ± 30; 1908 ± 8; 1998 ± 3		180 ± 40; 250^{+120}_{-50}; 101 ± 14; $359 \pm 10 \pm 3$	
Br(πN)	$3 \pm 2\%$		
Br($\Delta\pi_{L=1}$)	$17 \pm 8\%$	Br($\Delta\pi_{L=3}$)	$33 \pm 12\%$
Br($N(1520)\pi$)	$15 \pm 8\%$	Br($N\sigma$)	$4 \pm 3\%$
$A^{1/2}_{BW}$	0.024 ± 0.014	$A^{3/2}_{BW}$	-0.067 ± 0.030

conclude that $N(1900)3/2^+$ formation and decay leads to the observed pattern.

These observations made directly from the data are confirmed by the Bonn–Gatchina (BnGa) multi-channel partial wave analysis which includes a large number of pion and photo-induced reactions in addition to the data presented here. Compared to [23], further data were included in the BnGa-PWA [24]; including [21,25–27] as well as our recently published double polarization data [28–31]. The new analysis returns $N(1900)3/2^+$ properties which are well consistent with the values reported in [12,23] but inconsistent with the high precision mass and width claimed in [32,33]. The results are summarized in Table 1.

The result of a mass scan in which a single Breit–Wigner amplitude with $J^P = 3/2^+$ is added above $N(1720)\ 3/2^+$ to the set of amplitudes is shown in Fig. 4. In the scan the mass of the added $J^P = 3/2^+$-state is fixed while all other parameters are fitted freely. The χ^2-difference which is normalized to the minimal χ^2 of the fit shows a clear minimum in the respective mass range. The same is true if the χ^2-change due to the $p\pi^0\pi^0$ contribution

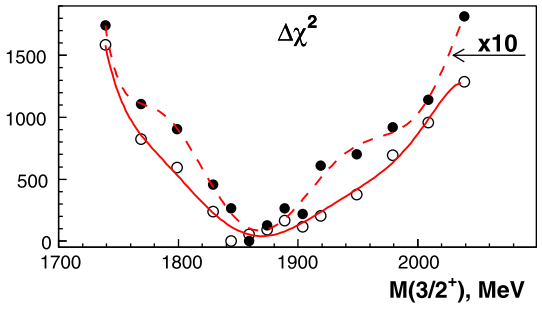

Fig. 4. Mass scan for a resonance with $J^P = 3/2^+$. Shown is the χ^2-change of the BnGa fit as a function of the imposed mass. In the mass scan, a Breit–Wigner amplitude with $J^P = 3/2^+$ is added above $N(1720)3/2^+$; its mass is fixed while all other parameters are fitted freely. The curves are included to guide the eye. The open circles give the total change in χ^2, normalized to the minimal χ^2. The black circles represent the χ^2 contribution from $p\pi^0\pi^0$; it is multiplied by a factor 10 for better visibility. The $\gamma p \to p\pi^0\pi^0$ data are fitted by an event-based likelihood fit; the likelihood $\mathcal{L}$ is converted into a pseudo-χ^2 by $\Delta(\ln\mathcal{L}) = 2\Delta\chi^2$.

only is plotted. The data on $\gamma p \to p\pi^0\pi^0$ and other three-body reactions are fitted within the BnGa-PWA by an event-based maximum likelihood fit. In this case the likelihood $\mathcal{L}$ is converted into a pseudo-χ^2 by $\Delta(\ln\mathcal{L}) = 2\Delta\chi^2$. A sizable fraction of $N(1520)3/2^-$ produced by photons in the 1300 to 1650 MeV energy range stems from decays of the $N(1900)3/2^+$ resonance.

The analysis presented here confirms the evidence for the existence of a second N^* with $J^P = 3/2^+$ at about 1900 MeV as suggested in [34]. That analysis was based on data on $K^+\Lambda$ pho-

toproduction [35–38] and other reactions. However, only the properties of the first resonance, $N(1900)3/2^+$, were well defined. The new data underline the need for a second N^* with $3/2^+$ but still, the properties of this second $3/2^+$ resonance remain uncertain; in some solutions its mass is found above, in other solutions below $N(1900)3/2^+$. If this second resonance is left out in the fit, the parameters of all resonances in this mass region change slightly, not only those of $N(1900)3/2^+$. These changes are included in the quoted error bars.

4. Summary

Summarizing, we have reported a measurement of two polarization observables I^s and I^c which govern polarization phenomena in photoproduction of three-body final states with linearly polarized photons. In the reaction $\gamma p \to p\pi^0\pi^0$ and with $N(1520)3/2^-$ as intermediate isobar, the pattern of I^s and I^c strongly suggests $J^P = 3/2^+$ as the primary partial wave at $\approx$1900 MeV in this reaction even without performing a partial wave analysis. The BnGa partial wave analysis confirms that the process $\gamma p \to N^* \to N(1520)3/2^-\pi^0 \to p\pi^0\pi^0$ receives large contributions from the $N(1900)3/2^+$ resonance. $N(1900)3/2^+$ belongs to a quartet of resonances which are incompatible with a quark–diquark picture of baryon excitations [39], and to the very few nucleon resonances for which a cascade decay via a nucleon resonance above the Roper resonance $N(1440)$ are reported.

Acknowledgements

We thank the technical staff of ELSA, the polarized target group, and the participating institutions for their invaluable contributions to the success of the experiment. We acknowledge support from the *Deutsche Forschungsgemeinschaft* (SFB/TR16), *Schweizerischer Nationalfonds* (200020-132799, 121781, 117601, 113511), *U.S. National Science Foundation* (NSF 0754674), and the RFBR (Grant 13-02-00425).

References

[1] K.A. Olive, et al., Chin. Phys. C 38 (2014) 090001.
[2] G. Höhler, et al., Physics Data, No. 12-1 (1979).
[3] R.E. Cutkosky, et al., in: 4th Int. Conf. on Baryon Resonances, Toronto, Canada, Jul 14–16, 1980. Publ. in: Baryon 19 (1980) (QCD161:C45:1980).
[4] R.A. Arndt, et al., Phys. Rev. C 74 (2006) 045205.
[5] S. Capstick, N. Isgur, Phys. Rev. D 34 (1986) 2809.
[6] U. Löring, et al., Eur. Phys. J. A 10 (2001) 395.
[7] R.G. Edwards, et al., Phys. Rev. D 84 (2011) 074508.
[8] E. Klempt, J.-M. Richard, Rev. Mod. Phys. 82 (2010) 1095.
[9] V. Crede, W. Roberts, Rep. Prog. Phys. 76 (2013) 076301.
[10] V.D. Burkert, Int. J. Mod. Phys. Conf. Ser. 26 (2014) 1460050.
[11] D.M. Manley, E.M. Saleski, Phys. Rev. D 45 (1992) 4002.
[12] V.A. Nikonov, et al., Phys. Lett. B 662 (2008) 245.
[13] A.V. Anisovich, et al., Phys. Lett. B 711 (2012) 167.
[14] W. Hillert, Eur. Phys. J. A 28 (2006) 139.
[15] F.A. Natter, et al., Nucl. Instrum. Methods B 211 (2003) 465.
[16] D. Elsner, et al., Eur. Phys. J. A 39 (3) (2009) 373.
[17] E. Aker, et al., Nucl. Instrum. Methods A 321 (1992) 69.
[18] R. Novotny, IEEE Trans. Nucl. Sci. 38 (1991) 379–385.
[19] E. Gutz, et al., Eur. Phys. J. A 50 (2014) 74.
[20] H. van Pee, et al., Eur. Phys. J. A 31 (2007) 61.
[21] V. Sokhoyan, et al., High statistics study of the reaction $\gamma p \to p\,2\pi^0$, in preparation.
[22] W. Roberts, T. Oed, Phys. Rev. C 71 (2005) 055201.
[23] A.V. Anisovich, et al., Eur. Phys. J. A 48 (2012) 15.
[24] A.V. Anisovich, et al., Eur. Phys. J. A 49 (2013) 158.
[25] M. Dugger, et al., Phys. Rev. C 88 (6) (2013) 065203;
M. Dugger, et al., Phys. Rev. C 89 (2) (2014) 029901 (Addendum).
[26] T.C. Jude, et al., Phys. Lett. B 735 (2014) 112.
[27] P. Aguar-Bartolome, et al., Phys. Rev. C 88 (4) (2013) 044601.
[28] A. Thiel, et al., Phys. Rev. Lett. 109 (2012) 102001;
R.L. Workman, M.W. Paris, W.J. Briscoe, I.I. Strakovsky, Phys. Rev. Lett. 110 (2013) 169101;
A. Thiel, et al., Phys. Rev. Lett. 110 (2013) 169102.
[29] M. Gottschall, et al., Phys. Rev. Lett. 112 (2014) 012003.
[30] J. Hartmann, H. Dutz, et al., Phys. Rev. Lett. 113 (2014) 062001.
[31] J. Hartmann, et al., The polarization variables T, P, and H and their impact on $\gamma p \to p\pi^0$ multipoles, in preparation.
[32] M. Shrestha, D.M. Manley, Phys. Rev. C 86 (2012) 055203.
[33] V. Shklyar, H. Lenske, U. Mosel, Phys. Rev. C 87 (1) (2013) 015201.
[34] A.V. Anisovich, et al., Eur. Phys. J. A 47 (2011) 27.
[35] R.G.T. Zegers, et al., Phys. Rev. Lett. 91 (2003) 092001.
[36] A. Lleres, et al., Eur. Phys. J. A 31 (2007) 79.
[37] A. Lleres, et al., Eur. Phys. J. A 39 (2009) 149.
[38] M.E. McCracken, et al., Phys. Rev. C 81 (2010) 025201.
[39] A. Thiel, et al., Phys. Rev. Lett. 114 (2015) 091803.